NASA

MEMORANDUM

INVESTIGATION OF SEVERAL BLUNT BODIES

TO DETERMINE TRANSONIC AERODYNAMIC CHARACTERISTICS

INCLUDING EFFECTS OF SPINNING AND OF EXTENDIBLE

AFTERBODY FLAPS AND SOME MEASUREMENTS

OF UNSTEADY BASE PRESSURES

By Lewis R. Fisher and Joseph R. DiCamillo

Langley Research Center
Langley Field, Va.

NATIONAL AERONAUTICS AND SPACE ADMINISTRATION

WASHINGTON
January 1959

NATIONAL AERONAUTICS AND SPACE ADMINISTRATION

MEMORANDUM 1-21-59L

INVESTIGATION OF SEVERAL BLUNT BODIES

TO DETERMINE TRANSONIC AERODYNAMIC CHARACTERISTICS

INCLUDING EFFECTS OF SPINNING AND OF EXTENDIBLE

AFTERBODY FLAPS AND SOME MEASUREMENTS

OF UNSTEADY BASE PRESSURES*

By Lewis R. Fisher and Joseph R. DiCamillo

SUMMARY

Several blunt bodies having shapes that may be suitable for atmospheric reentry vehicles were tested to determine the aerodynamic characteristics of such shapes for angles of attack up to 34°. The tests were conducted through the transonic Mach number range and at Reynolds numbers from 1.74×10^6 to 2.78×10^6, based on body diameter.

A full-skirted rather than a short-skirted type of shape developed the greatest amount of static stability and the largest lift-curve slopes. The angle of attack for maximum lift for such bodies appears to be subject to Mach number effects. Spinning a full-skirted body about its longitudinal axis generally increased the lift and reduced the pitching moment at angles of attack and reduced the aerodynamic static stability parameter through the transonic Mach number range. The extension of segmented clamshell-shaped flaps from the afterbody of a short-skirted model served to increase the lift and static stability only if the flaps extended into the airstream.

Some evidence was found of oscillatory base pressures on two dissimilar shapes at certain high angles of attack and the highest Mach number in these tests. There is doubt, however, that these pressures can induce any significant oscillatory motion for a reentry vehicle because of their small amplitude and phasing.

---

*Title, Unclassified.

INTRODUCTION

Reference 1 presents the results of a transonic wind-tunnel investigation of the aerodynamic characteristics of several families of blunt bodies. These body shapes were deemed to be suitable for use as atmospheric reentry vehicles because blunt bodies have been shown (ref. 2) to have significantly lower convective heat-transfer rates at the stagnation region than sharp-nosed shapes. The present investigation forms an extension of the investigation reported in reference 1 in that three bluff shapes similar to some of those described in reference 1 were tested through a larger angle-of-attack range than was possible in the previous investigation. In addition, these three basic models (sometimes with modifications) were tested in order to determine the effects of spinning and of extendible afterbody flaps and to measure fluctuating base pressures on two dissimilarly shaped models. Also, a right circular cone with a sharp nose and one with a slightly blunt nose were tested for comparison purposes. These tests were conducted in the Langley 8-foot transonic pressure tunnel for Mach numbers between 0.7 and 1.15 and Reynolds numbers between 1.74×10^6 and 2.78×10^6, based on body diameters of 6 and 8 inches.

SYMBOLS

The data are referred to the stability system of axes (fig. 1) and are presented in the form of coefficients of forces and moments about a point one-third of the length of the model rearward from the front face. The coefficients and symbols used are defined as follows:

C_D drag coefficient, $\dfrac{\text{Drag}}{qS}$

C_{D_o} drag coefficient at zero lift

C_L lift coefficient, $\dfrac{\text{Lift}}{qS}$

C_m pitching-moment coefficient, $\dfrac{\text{Pitching moment}}{qSd_{max}}$

$C_{L_\alpha} = \dfrac{\partial C_L}{\partial \alpha}$, per radian

L-180

$$C_{m_\alpha} = \frac{\partial C_m}{\partial \alpha}, \text{ per radian}$$

d   diameter of model, ft

M   free-stream Mach number

q   free-stream dynamic pressure, lb/sq ft

R   Reynolds number, based on body diameter

r   radius

S   maximum cross-sectional area of model, sq ft

α angle of attack, deg

Subscript:

max   maximum

APPARATUS AND TESTS

Apparatus

The models shown in figure 2 represent the configurations tested. Models 1 and 1s were geometrically similar; however, model 1 was mounted statically on the sting, whereas model 1s was mounted on bearings which permitted freedom of rotation about the longitudinal axis as shown in figure 2(c). Models 2 and 3 were short-skirted shapes, of which model 3 had the more rounded and shallower forebody. Models 3a and 3b were formed from model 3 by simulating extendible flaps opening in clamshell fashion from the model afterbody. The flaps of model 3a were one-half the length of the afterbody and those of model 3b were the entire length. Both sets of flaps formed an angle of 50° with the original afterbody surface. In addition to these models, two cones of 15° total included vertex angle were tested. One cone had a sharp nose and the other had a nose which was only slightly rounded.

In order to provide measurements of any fluctuations in base pressure, four pressure transducers of 2 pounds per square inch capacity were arranged 90° apart on the bases of models 1 and 2. The electrical signals from the transducers were read by means of a recording oscillograph.

Model 1s was forced to spin at rotational speeds up to 1,800 revolutions per minute, during testing, by compressed air at approximately 90 pounds per square inch pressure directed against a small turbine wheel built into the base of the model. (See fig. 2(c).) The air jets were oriented as closely as possible along the transverse model axis in order to minimize any longitudinal forces on the model because of the jets. The compressed air was carried into the test section from an external source by means of 1/4-inch-diameter tubing through the sting support and along the outside of the sting to a point directly behind the base of the model. The model rotation was controlled by a manually operated valve in the airline outside the test section. In order to measure the speed of rotation, a small magnet was imbedded in the base of the model, and a wire coil was fixed to the sting so that the movement of the magnet past the coil induced a current in the coil. These signals were then read visually on a time-interval counter.

The models were sting mounted in the Langley 8-foot transonic pressure tunnel. The test section of this tunnel is rectangular in cross section and has upper and lower walls which are slotted to permit continuous operation through the transonic speed range up to a Mach number of 1.20. Forces and moments on the models were measured by means of a six-component wire strain-gage balance. A portion of this balance which extended beyond the model was protected from the airstream by a windshield. The data were recorded on punched cards during the tests.

Tests

The angle-of-attack range of this investigation was covered during two separate groups of tests. The first tests were for the range of $\alpha = 0°$ to $\alpha = 24°$; the second were made with a bent sting coupling and were for the range of $\alpha = 24°$ to $\alpha = 34°$. The tests were made at Mach numbers of 0.70, 0.90, 0.95, 1.00, and 1.15 and Reynolds numbers between 1.74×10^6 and 2.78×10^6, based on model diameters of 6 and 8 inches; the relationship of Mach number and Reynolds number is shown in figure 3. The wind tunnel was operated at a stagnation pressure of 1 atmosphere and a stagnation temperature of $124°$ F.

During the tests of models 1 and 2, the fluctuating base pressures were recorded for 10-second intervals for each angle of attack and Mach number. During the testing of the spinning model, efforts were made to hold the rotational speed of the model as closely as possible to an arbitrarily selected value of 1,800 revolutions per minute. However, the varying aerodynamic loadings caused by the changes in angle of attack and the varying bearing loads resulted in rotational speeds which were often considerably below the desired value with the maximum supply of air available.

RESULTS AND DISCUSSION

Presentation of Results

For the presentation of the test results, the measured normal and axial forces were converted to lift and drag forces and are presented as lift and drag coefficients. The measured data included the lateral force and the rolling and yawing moments; because of the axial symmetry of the models, however, the lateral coefficients were at all times approximately zero and are not presented herein.

The variations of the lift, drag, and pitching-moment coefficients with angle of attack for the eight models tested are presented as figures 4 to 11. Figures 12 to 14 are comparison figures for related models and indicate the variations of C_L and C_m with Mach number for certain angles of attack. The slopes C_{L_α} and C_{m_α} and the drag coefficient at zero lift are shown as functions of Mach number in figures 15 to 18 for the related models.

Variations With Angle of Attack

The results of the present investigation are consistent with those of reference 1, in that the models with the greatest amount of skirt surface area (model 1 and the cone models) exhibited the highest lift-curve and static-stability slopes.

In the case of model 1 (fig. 4), and to some extent model 3 (fig. 7), the lift increased positively with angle of attack until some angle was attained where the lift decreased very markedly. This event, which was also reflected as a decrease in the magnitude of the pitching moment, occurred for only the lower Mach numbers for which the initial lift-curve slopes were the highest. The abrupt reduction in lift is probably the result of shock-induced separation and an associated reduction in suction pressures on the upper surface of the body. For the highest Mach numbers, the pressure gradients on the upper surface of the body are less severe than at lower Mach numbers; the tendency toward separation is thereby reduced.

The data of figure 4 indicate that the angle of attack of maximum lift for model 1 is very much subject to Mach number and Reynolds number effects. Some unpublished results obtained in transonic tests at the Ames Research Center indicated that, for blunt bodies similar to those of this investigation, the lift and pitching-moment coefficients measured for increasing angles of attack differed significantly from the corresponding results measured for decreasing angles of attack and

that this effect tended to show some dependence upon Reynolds number. Such an aerodynamic hysteresis could be the result of the uncertainty the flow exhibits in regard to the angle of attack for separation.

The initial lift-curve slope for model 2 (fig. 6) also appears to be relatively sensitive to Mach number. Although the models are not entirely dissimilar, the same sensitivity is not shown by model 3 (fig. 7), however, probably because the face of model 3 is more rounded than that of model 2. Reference 1 also showed that a flat-faced model is more sensitive than a rounded-faced model to Reynolds number.

The variations of the aerodynamic coefficients with angle of attack for the spinning model (fig. 5) were not appreciably different from those of the nonspinning model (fig. 4), at least up to the highest angle of attack ($\alpha = 24^\circ$) at which model 1s was tested. The variations for models 3a and 3b (figs. 8 and 9) were also not very much different from those for the basic model 3 (fig. 7), with the exception that model 3b exhibited considerably more static stability and higher lift than did models 3 and 3a. The detailed effects of spin and of extendible flaps are discussed later.

Variations With Mach Number

The variation of the coefficients C_L and C_m with Mach number at selected angles of attack are shown for models 1 and 1s in figure 12, for models 3, 3a, and 3b in figure 13, and for the cone models in figure 14. Model 1 experienced some changes in both lift and pitching moment through the transonic speed range at angles of attack where the model developed lift. The spinning motion of model 1s did not change the trend of these variations. The transonic Mach number effects on the coefficients for model 3 were less severe than those for model 1 because model 3 did not develop the lift that model 1 did. The conical models, while developing a considerable amount of lift, showed relatively minor effects of Mach number in the transonic speed range (fig. 14). The angles of attack for the tests of the cone models were, however, limited by the very high pitching moments developed by these models and by the capacity of the strain-gage balance.

Of the models tested, model 1 and the cone models showed the largest effects of Mach number on the static stability (figs. 15 and 18). These are, of course, the models with the largest amounts of skirt area behind the center of gravity of the model. In the case of the cone models (fig. 18) the static stability was constant for $M = 0.9$ and higher Mach numbers. Blunting the sharp nose of the cone slightly had no effect on the variation of the coefficients with Mach number but did increase the static stability at all Mach numbers. The increase in stability was

apparently caused by a rearward shift in the center of pressure since the bluntness had no effect on the lift of the cone.

A model similar in shape to model 1, but with a somewhat flatter face, was tested in the investigation of reference 1; these results are included for comparison purposes in figure 15. Other results from reference 1 for two models similar in configuration to models 2 and 3 are included in figure 16.

Effect of Spinning

Model 1 was spun about its longitudinal axis at approximately 1,800 revolutions per minute in order to determine whether spinning could cause a rotation of the lift vector about the spin axis. Such an event would be indicated by an increase in the lateral force and possibly the yawing moment of the spinning model over those values for the nonspinning model. The test results indicate no such increases in either lateral force or yawing moment for the spinning model; hence, at 1,800 revolutions per minute at least, no rotation of the lift vector was detectable.

In the subsonic Mach number range the spinning did, however, effect an increase in lift at the higher angles of attack (fig. 12). In addition, the pitching-moment coefficients for the model were reduced for all angles of attack through the entire transonic Mach number range. Although there may have existed some separate effects of the air jet or of the spinning motion on drag, figures 4 and 5 show no appreciable differences in the net drag coefficients. The initial lift-curve slopes shown in figure 15 were not materially affected by the spinning, but the static stability C_{m_α} was reduced substantially through the Mach number range.

Effect of Extendible Flaps

The effects of the extension of segmented, clamshell-shaped flaps from the afterbody of model 3 on the lift and pitching-moment coefficients at selected angles of attack are shown in figure 13 and on C_{L_α}, C_{m_α}, and C_{D_0} in figure 17. The extension of the small flaps of model 3a resulted in no significant increments in any of the aerodynamic coefficients, probably because the flaps were always immersed in a region of separated flow behind the model. The larger flaps of model 3b extended well into the airstream, however, and provided large increments in pitching moment and in lift coefficient. The effectiveness of these flaps tended to increase as the angle of attack of the model increased and a greater portion of the lower flaps extended into the airstream while the

upper flaps became more immersed in the separated flow. Only at these high angles of attack was the drag very much higher for the model with the larger flaps than for the model without flaps. The static stability of model 3 was also increased by the use of the larger flaps, with the most significant increase taking place at the supersonic Mach numbers.

Oscillatory Base-Pressure Measurements

Pressure transducers were embedded in the bases of models 1 and 2, as indicated in figure 2, in order to measure the frequency and amplitude of any fluctuating pressures which may have been associated with a periodic type of flow separation. Cyclic pressures of this nature may induce an oscillatory yawing or pitching motion on the part of a reentry body.

An analysis of the pressure traces indicates that pressure oscillations occurred at only the conditions of the highest Mach number and some of the highest angles of attack tested. For model 1 at a Mach number of 1.15 one of the laterally opposed transducers recorded an oscillation in pressure starting at an angle of attack of approximately 24° and continuing with varying amplitude and frequency through an angle of attack of 34°. These oscillations were of the order of 0.1 pound per square inch in amplitude and 0.85 cycle per second in frequency. Unfortunately, the other laterally disposed transducer proved to be inoperative. The two vertically opposed transducers, however, gave no indication of pressure oscillations throughout the angle of attack and Mach number ranges tested.

Calculations have shown that the magnitude of the yawing moment induced by the amplitude of the pressure fluctuations for the maximum conditions was only 0.5 percent of the pitching moment and may, therefore, be considered negligible.

In the case of model 2 the first oscillations occurred at $M = 1.15$ and $\alpha = 30^\circ$ on two of the transducers located 90° apart on the rear face. At $\alpha = 34^\circ$, however, all four pressure orifices indicated oscillations. These oscillations appeared to be related in phase for approximately one-half of a 10-second run. The relationship was such that the upper and lower transducers and the one on the right side were in phase while the one on the left side was 180° out of phase with the group. The amplitude and frequency of these oscillations averaged 0.2 pound per square inch and 1.2 cycles per second.

These recorded fluctuations could not induce any pitching moment because of the fact that the vertically opposed pressure transducers were in phase with one another. The left and right transducers, however,

were out of phase, and calculations show that the maximum yawing moment induced was of the order of 2.5 percent of the pitching moment, which is somewhat larger than that calculated for model 1.

CONCLUSIONS

An investigation was conducted at transonic speeds to determine the aerodynamic characteristics at angles of attack up to $34°$ of several blunt bodies such as may be suitable for atmospheric reentry vehicles. Some effects of spin rate and of extendible clamshell-shaped flaps were measured in addition to the fluctuating base pressures on two of the models. The results of this investigation indicate the following conclusions:

1. As was found in a previous transonic investigation, the largest lift-curve and static-stability slopes were developed by the full-skirted rather than the short-skirted type of body. The angle of attack for maximum lift for the full-skirted body appears to be highly dependent upon Mach number and presumably upon Reynolds number, at least at the lower Mach numbers. The lift-curve slope of the body having the less rounded face also appears to be relatively sensitive to Mach number.

2. Spinning a blunt body about its longitudinal axis had the effect of generally increasing the lift and reducing the pitching moment at angles of attack and of reducing the aerodynamic static stability parameter of the body through the transonic range of Mach numbers.

3. The extension of segmented, clamshell-shaped flaps from the after-body of a short-skirted body served to increase the lift and static stability only if the flaps extended into the airstream.

4. Two dissimilarly shaped bodies showed some evidence of oscillatory base pressures at the highest Mach numbers and certain of the higher angles of attack. These pressures were small in amplitude, however, and phased so as to make it doubtful that any significant oscillatory motion could result from them.

Langley Research Center,
        National Aeronautics and Space Administration,
            Langley Field, Va., October 15, 1958.

REFERENCES

1. Fisher, Lewis R., Keith, Arvid L., Jr., and DiCamillo, Joseph R.:
   Aerodynamic Characteristics of Some Families of Blunt Bodies at
   Transonic Speeds. NASA MEMO 10-28-58L, 1958.

2. Allen, H. Julian, and Eggers, A. J., Jr.: A Study of the Motion and
   Aerodynamic Heating of Missiles Entering the Earth's Atmosphere at
   High Supersonic Speeds. NACA TN 4047, 1957. (Supersedes NACA
   RM A53D28.)
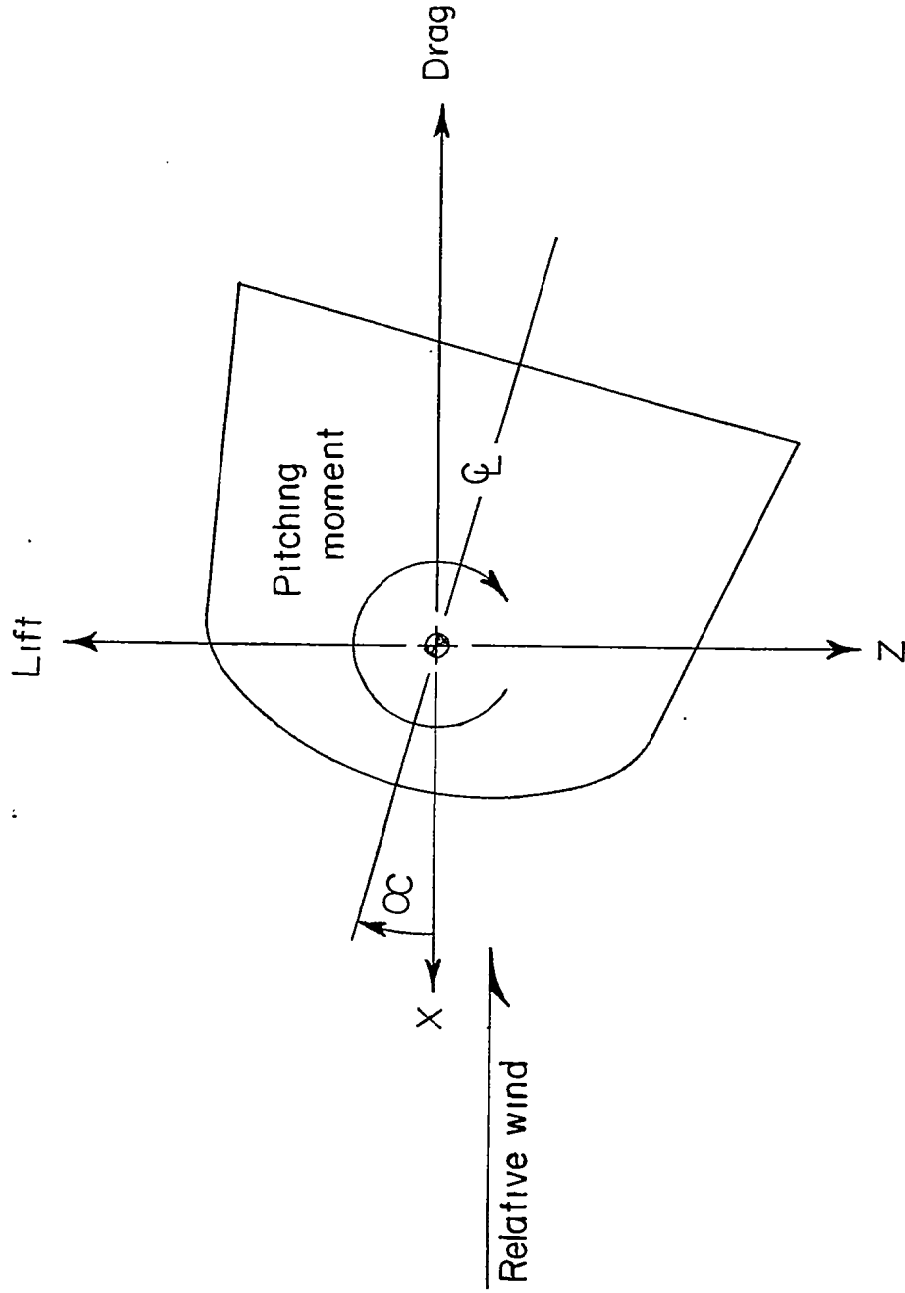
Figure 1.- System of stability axes. Arrows indicate positive directions of forces, moments, and angular displacements.
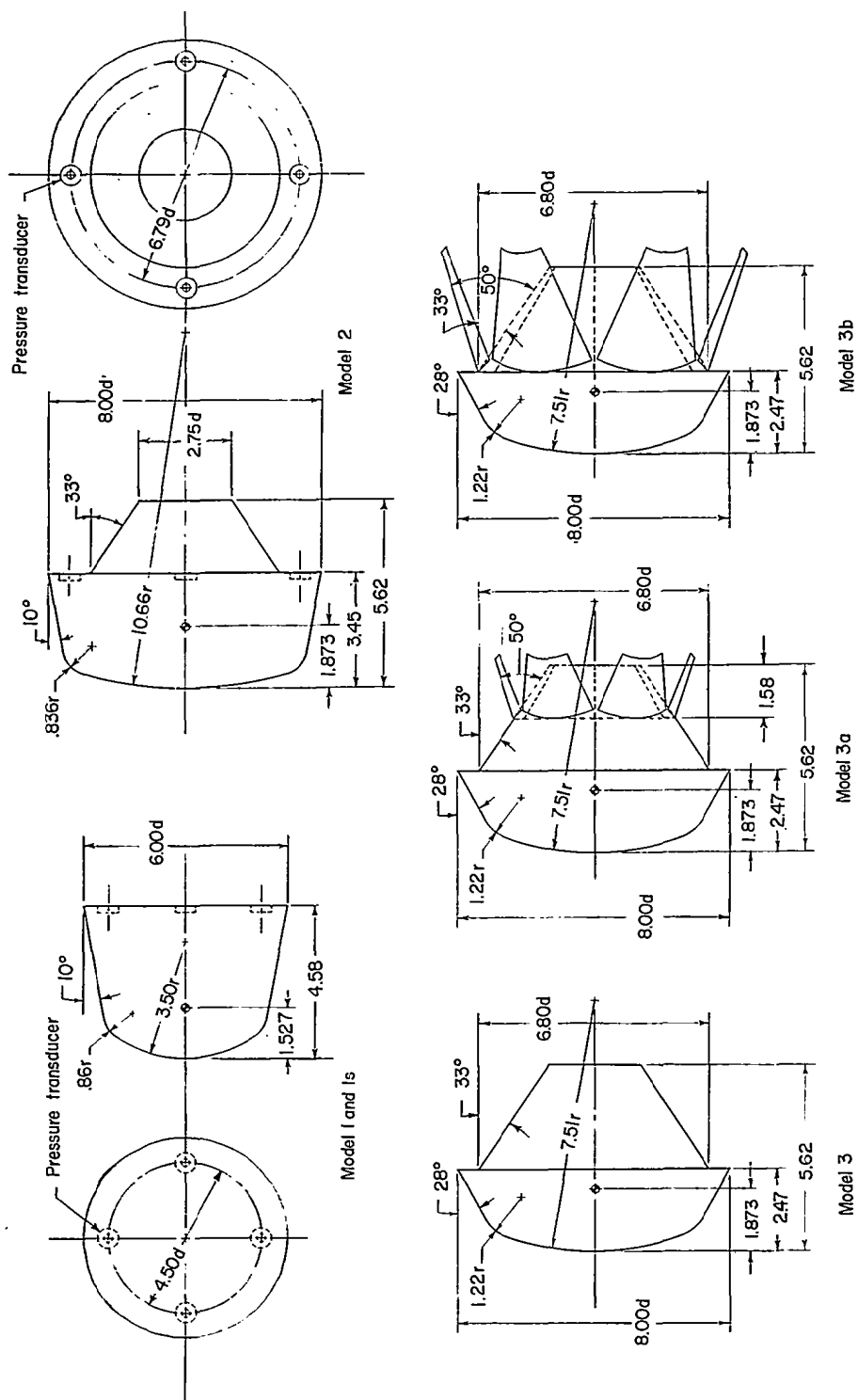
(a) Models 1, 2, and 3 with modifications thereto. All linear dimensions are in inches.

Figure 2.- Drawings of models tested.
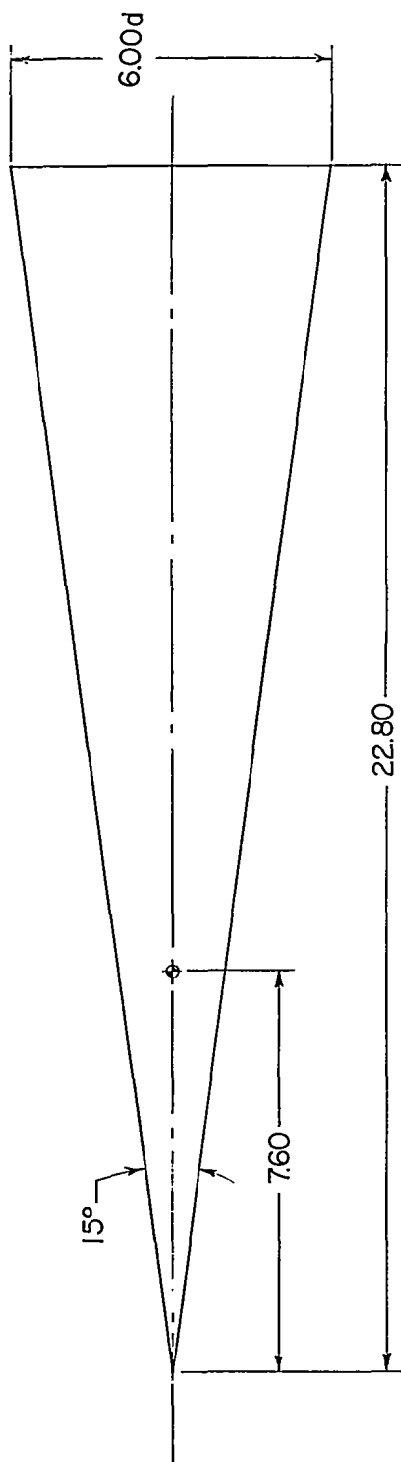
Sharp nose cone
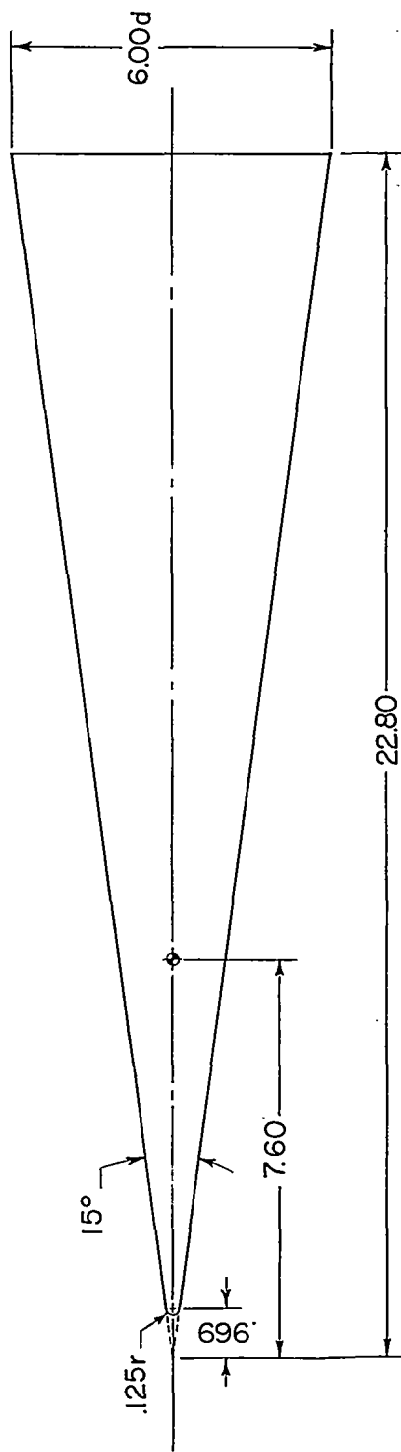
Blunt nose cone

(b) Cone models.

Figure 2.- Continued.

Air supply

Balance windshield

Sting balance

Air jets

Turbine blades

Bearings
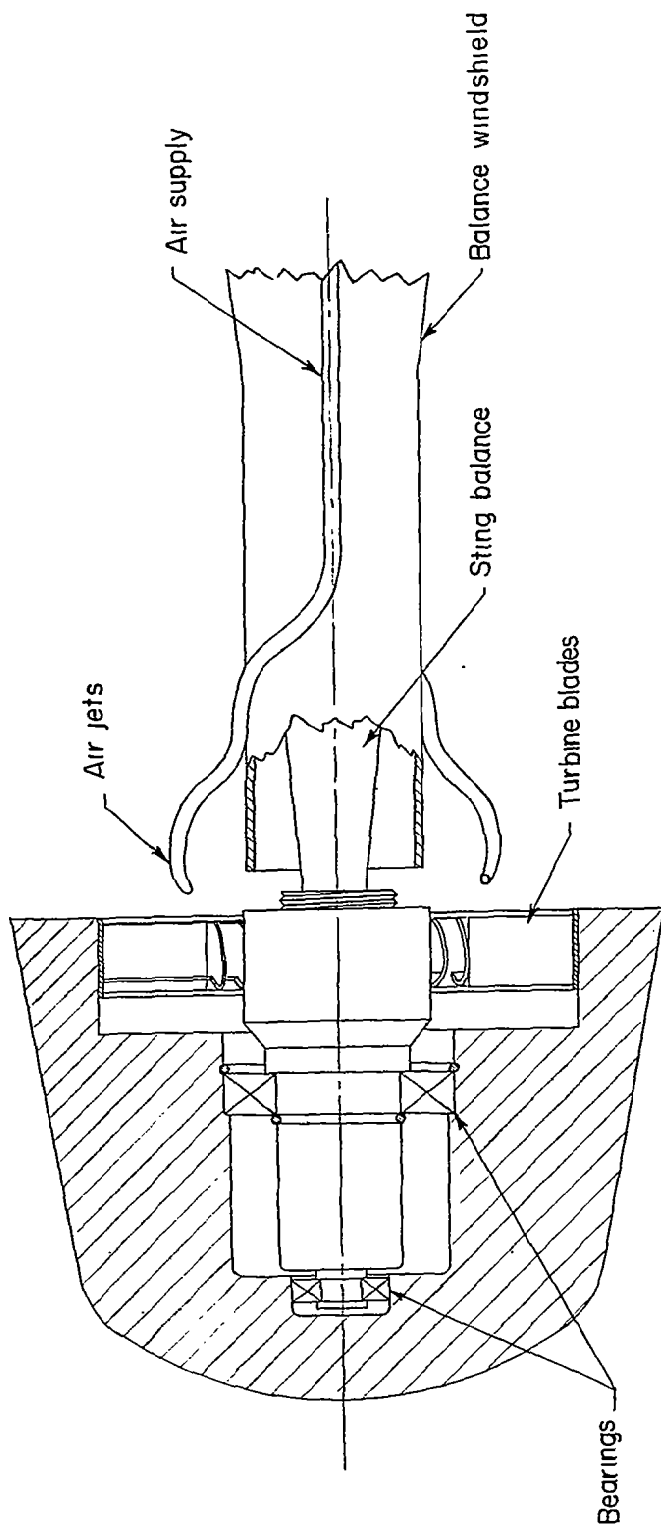
(c) Model 1s.

Figure 2.- Concluded.
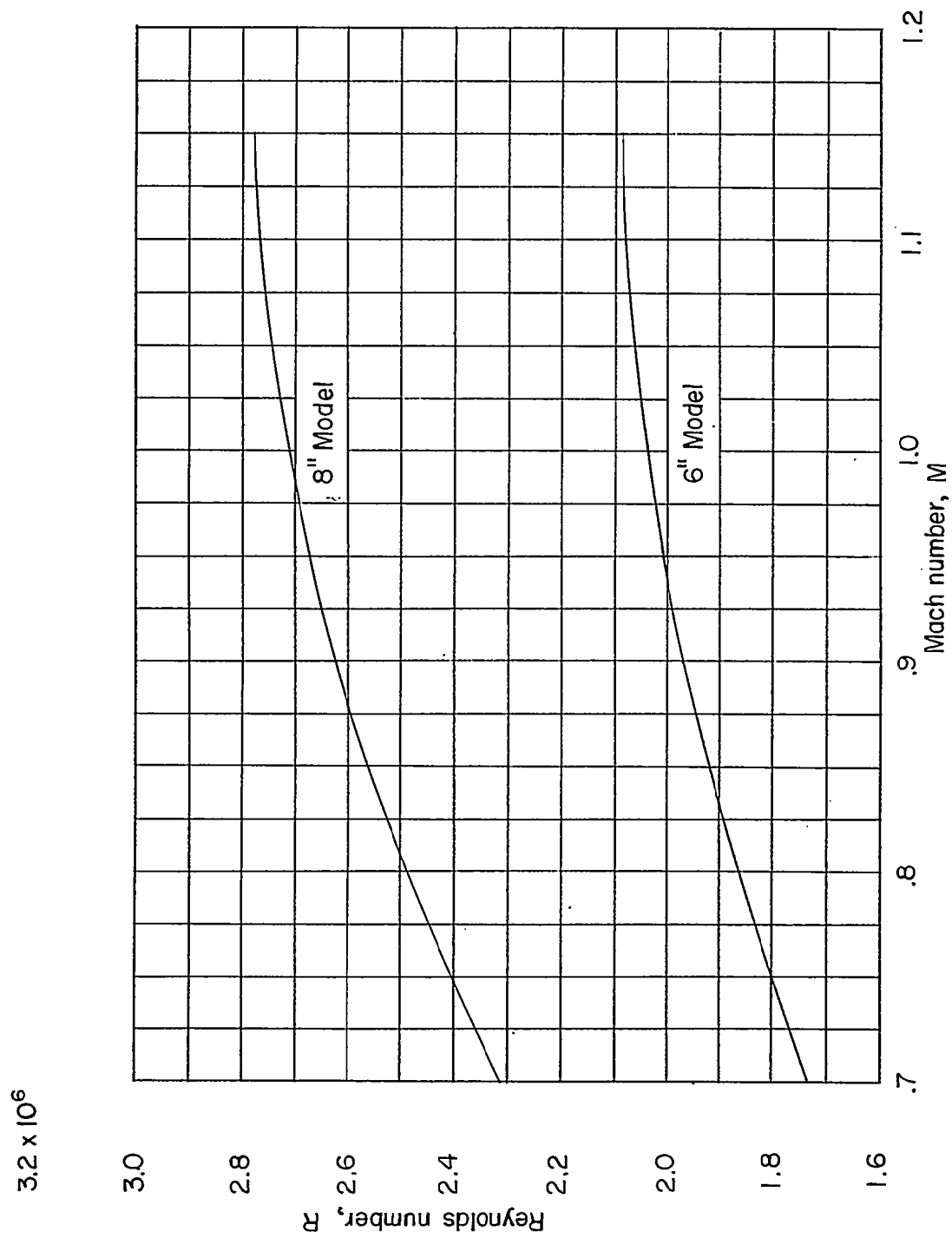
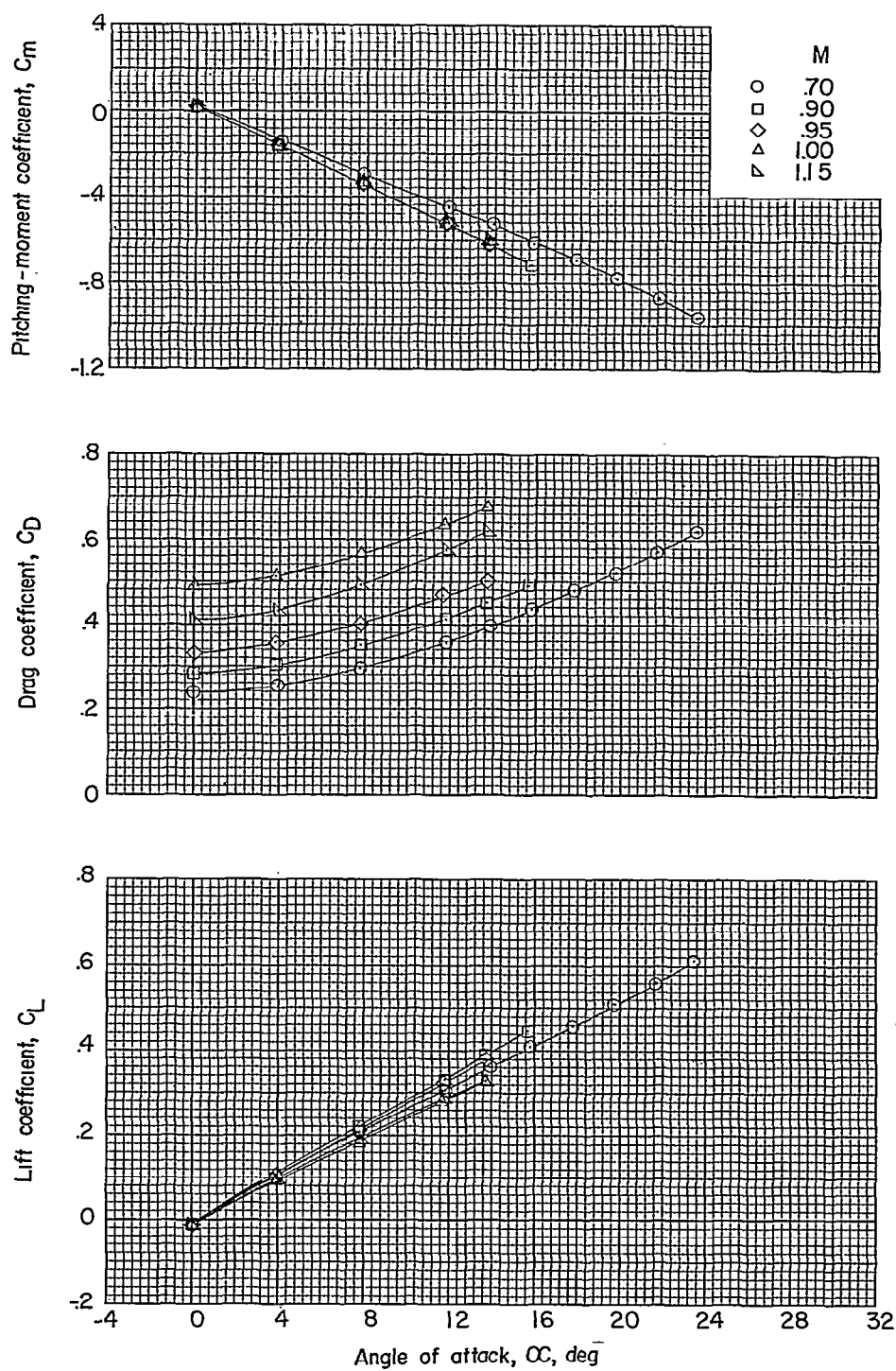Figure 3.- Variation of Reynolds number (based on body diameter) with Mach number.
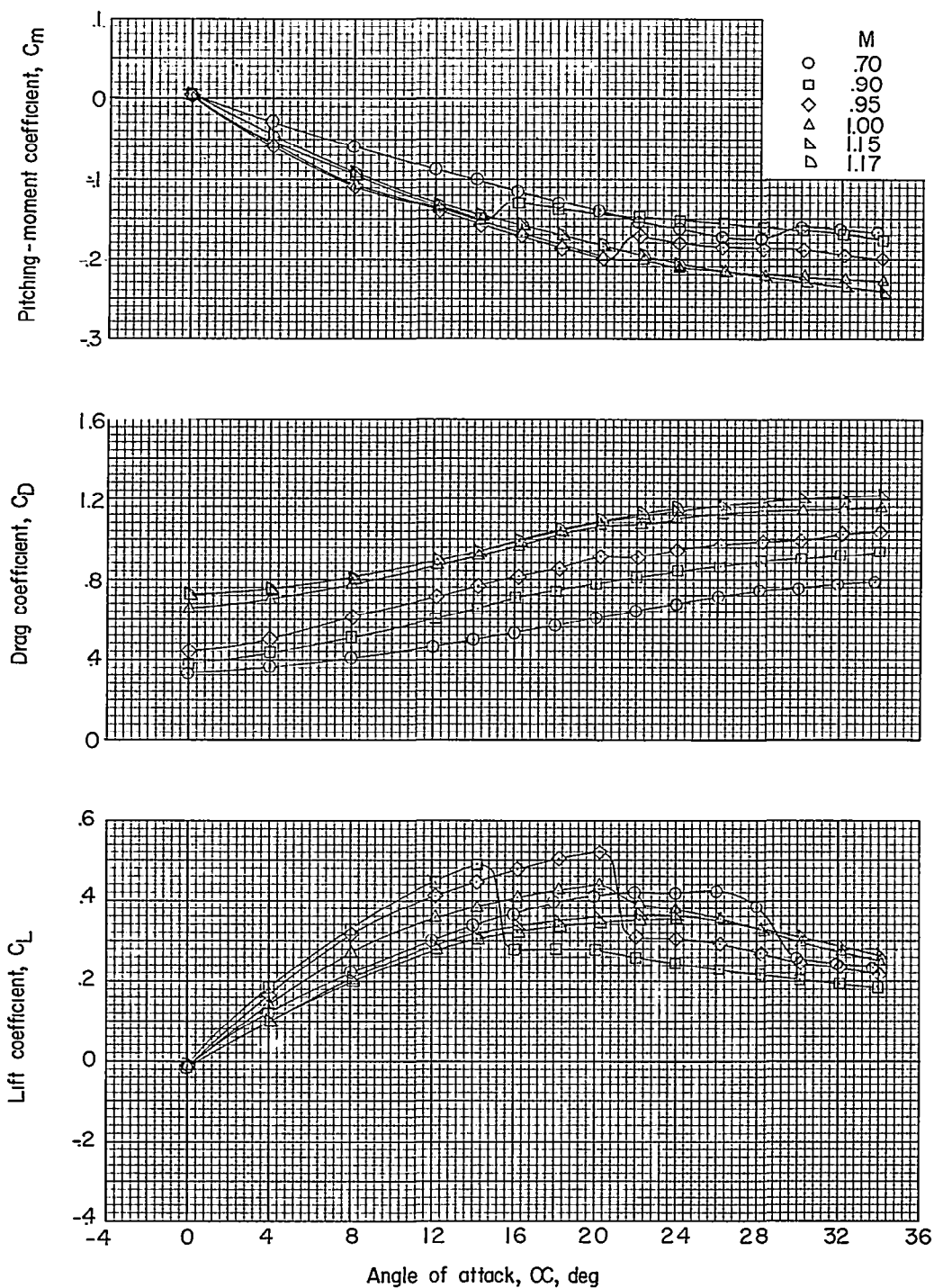
Figure 4.- Variation with angle of attack of lift, drag, and pitching-
moment coefficients for model 1.

L-180
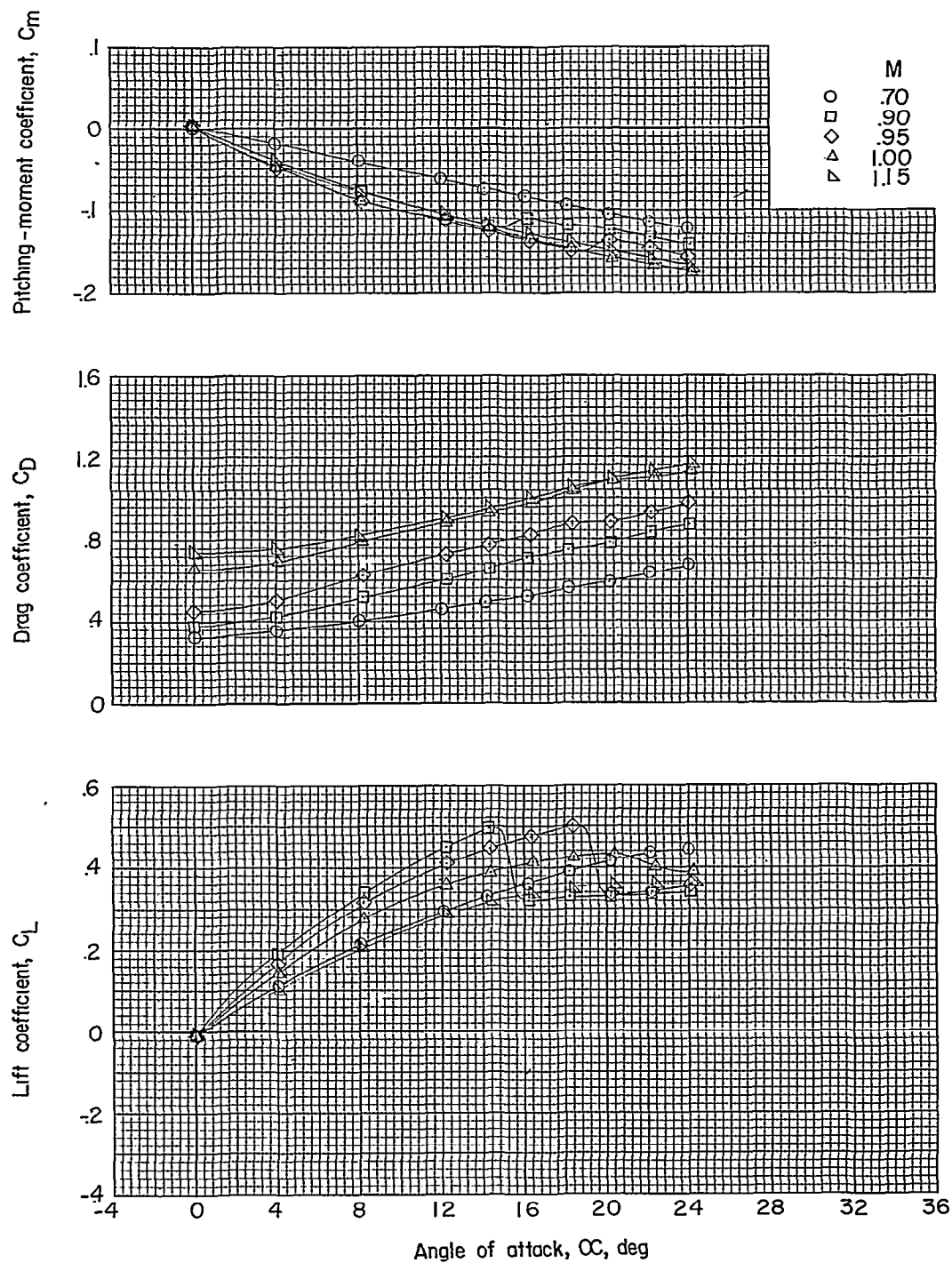
Figure 5.- Variation with angle of attack of lift, drag, and pitching-
moment coefficients for model 1s.
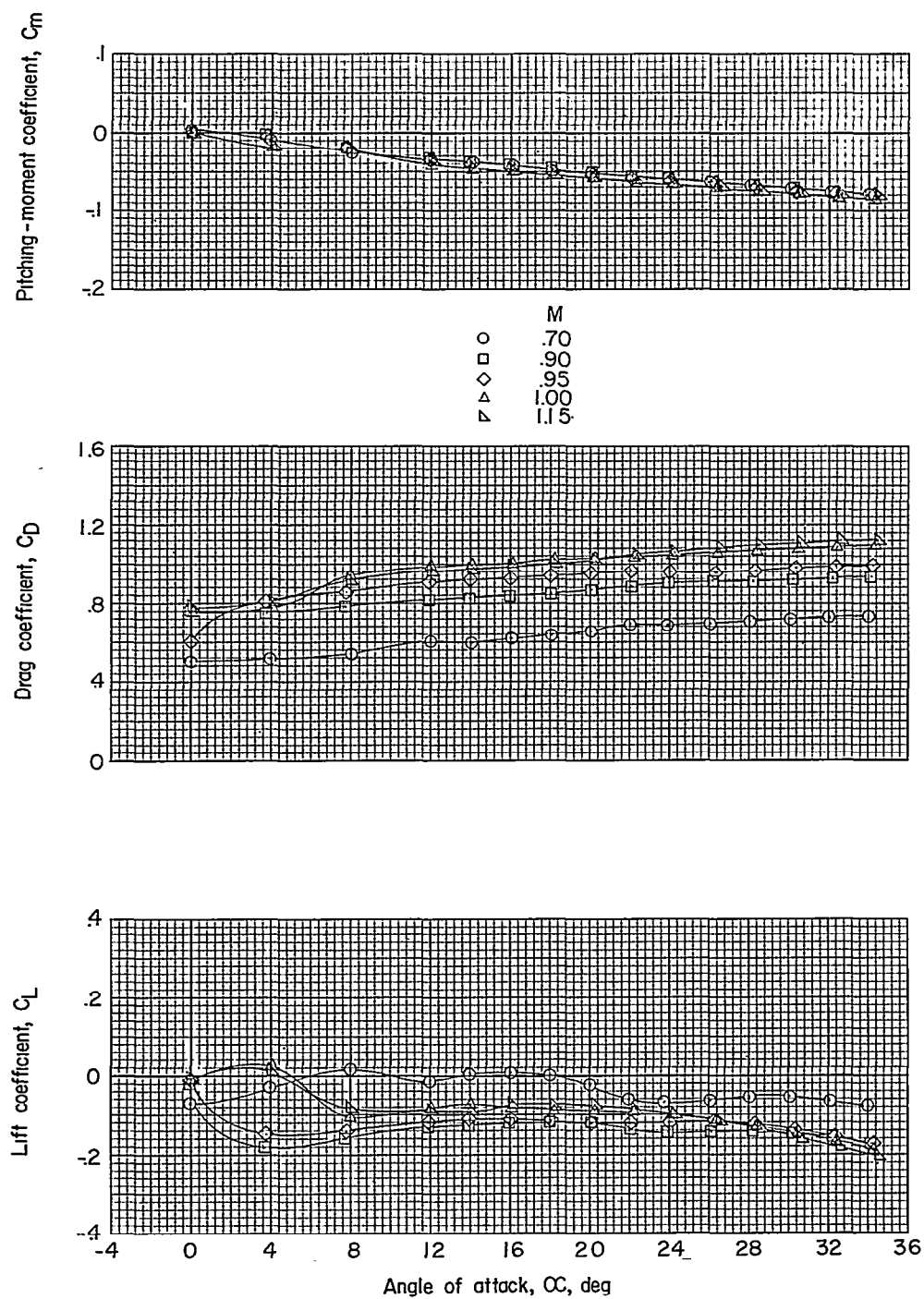
Figure 6.- Variation with angle of attack of lift, drag, and pitching-moment coefficients for model 2.

L-180
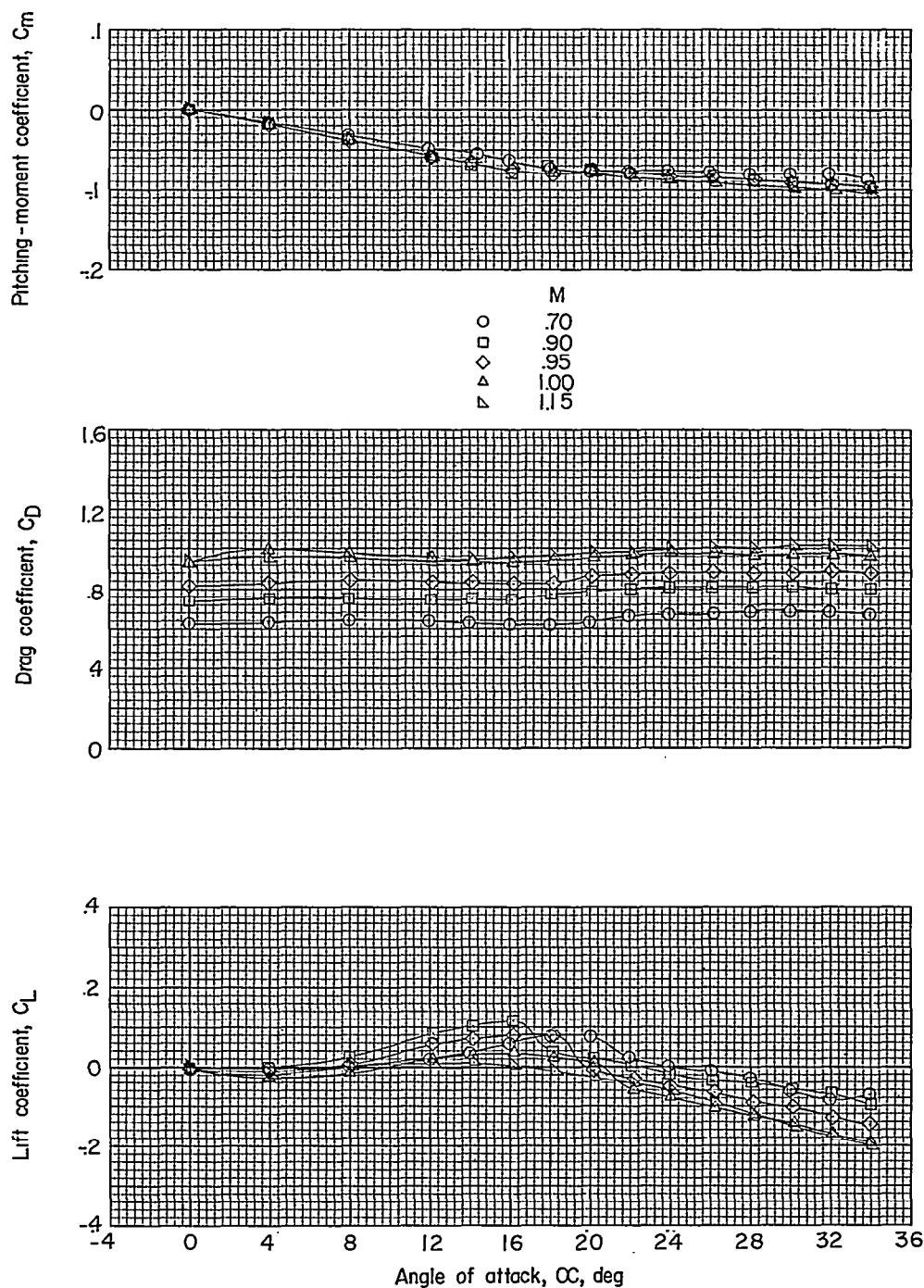
Figure 7.- Variation with angle of attack of lift, drag, and pitching-moment coefficients for model 3.
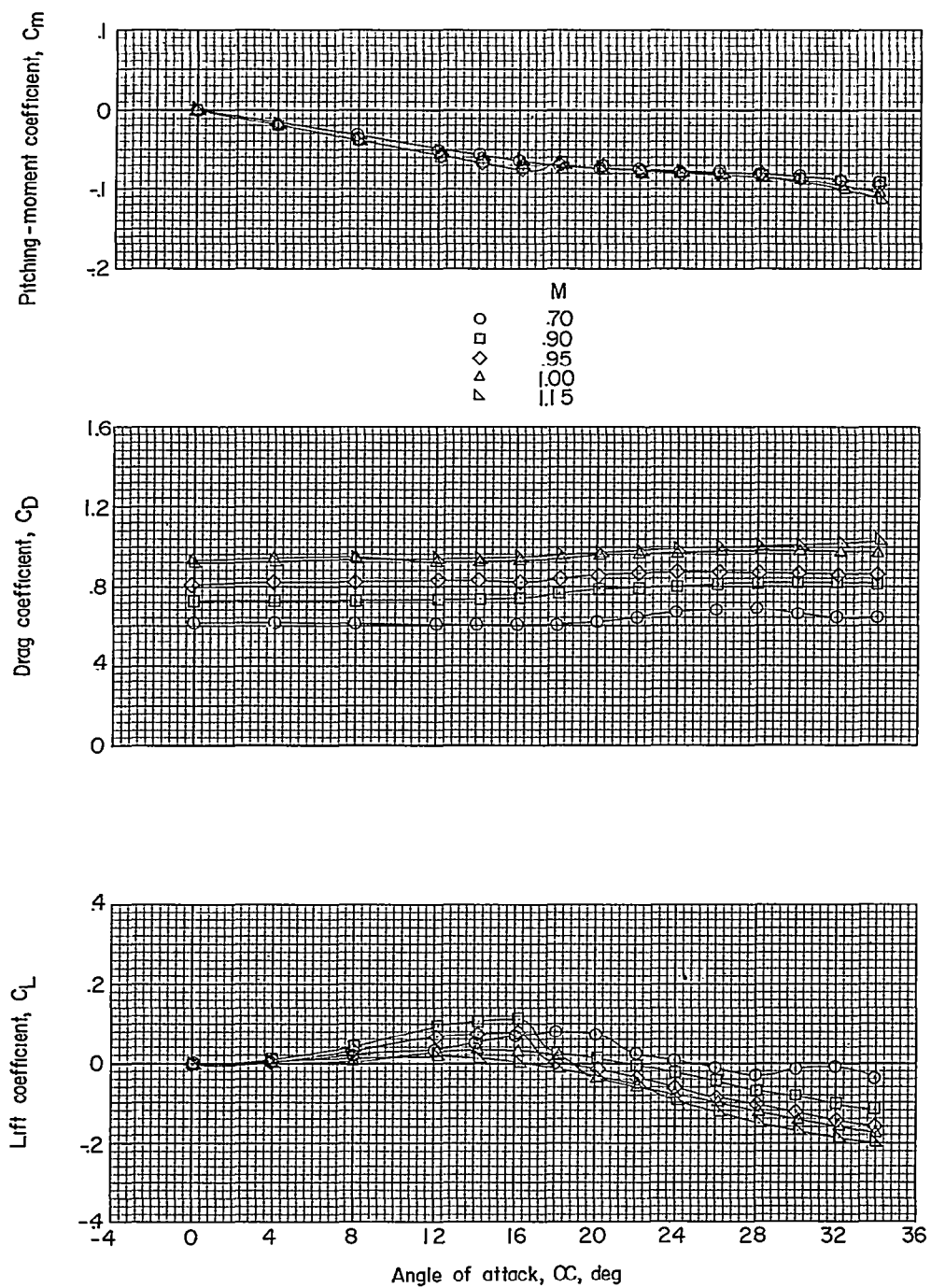
Figure 8.- Variation with angle of attack of lift, drag, and pitching-moment coefficients for model 3a.
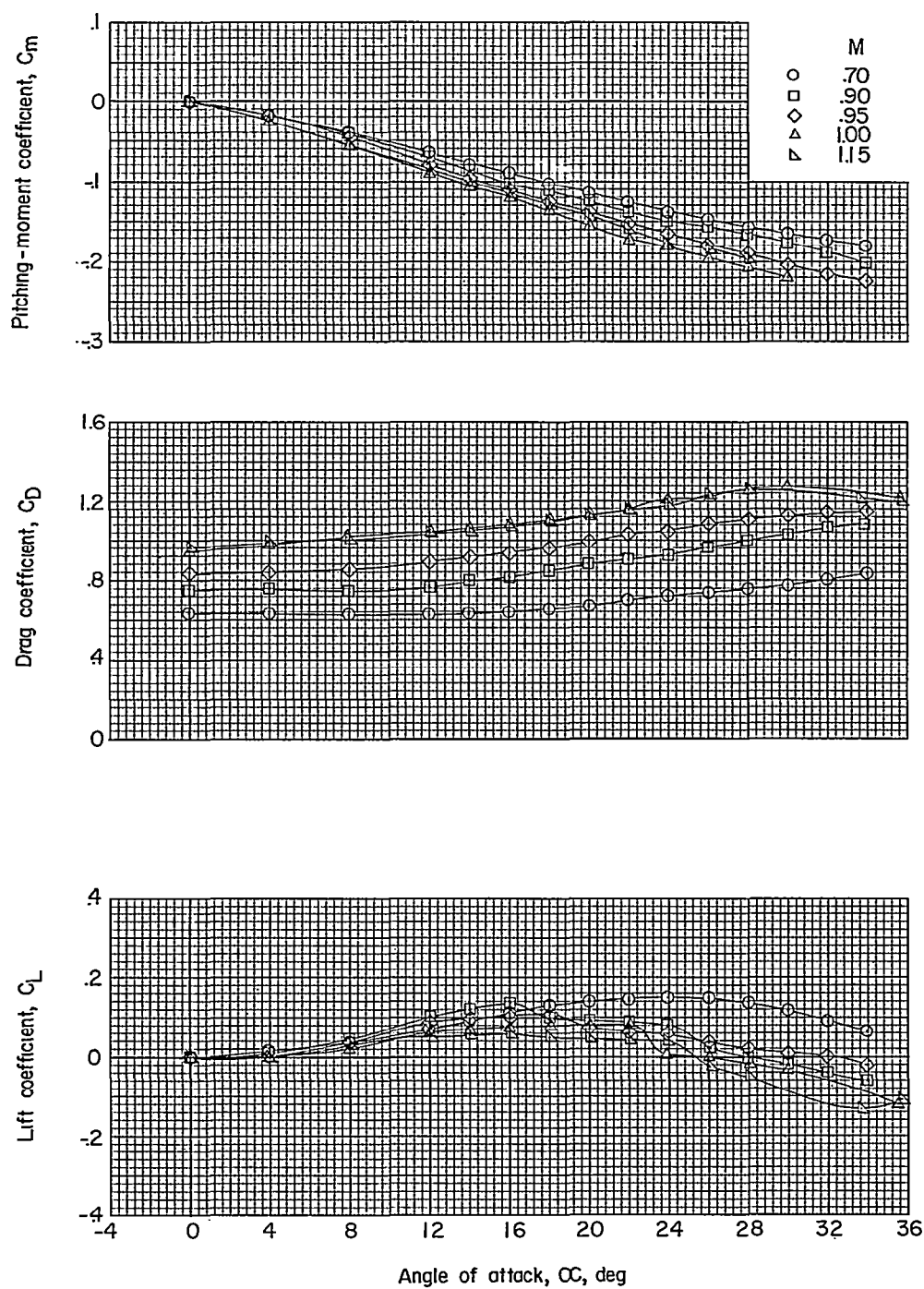
Figure 9.- Variation with angle of attack of lift, drag, and pitching-moment coefficients for model 3b.
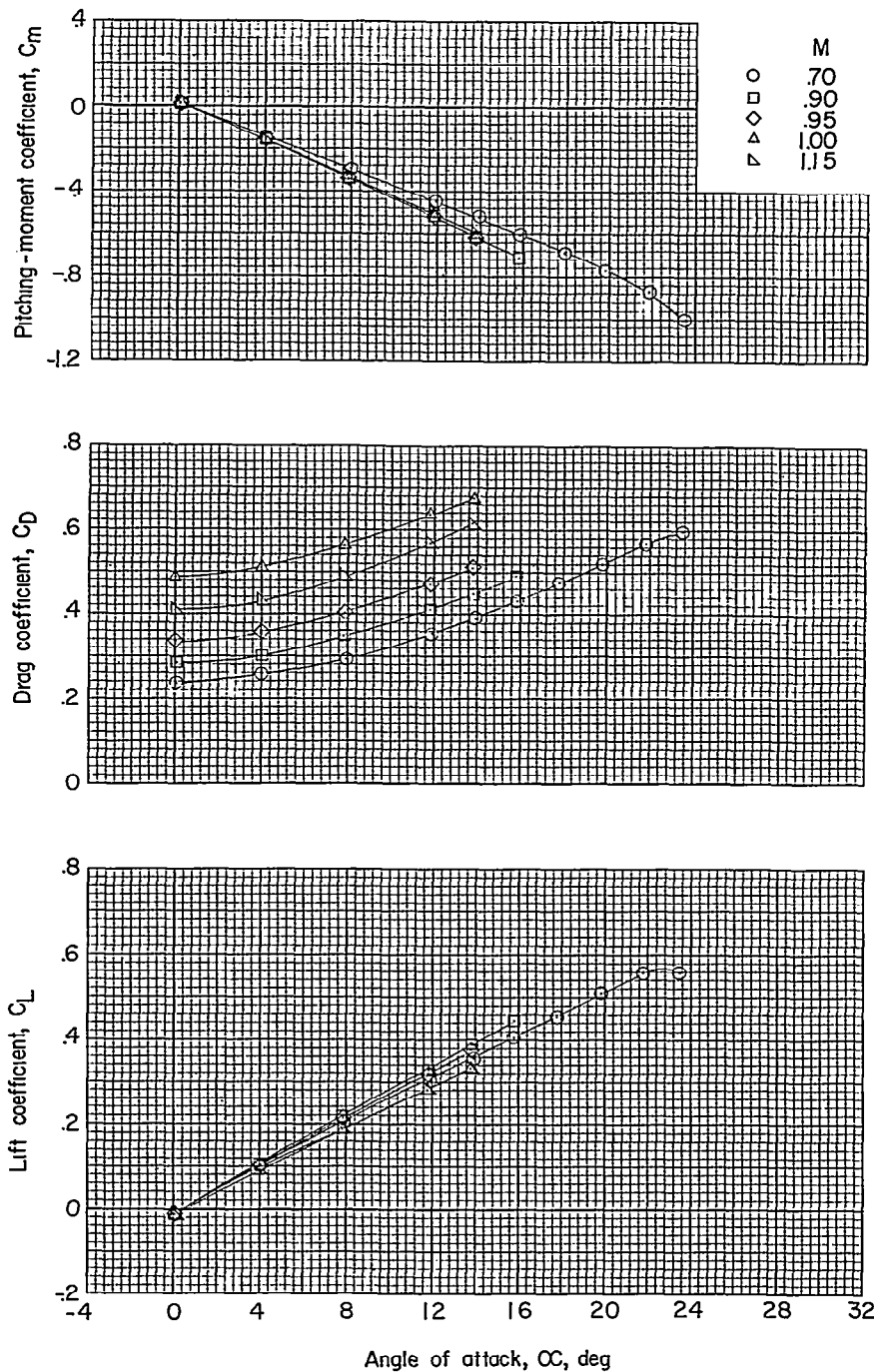
Figure 10.- Variation with angle of attack of lift, drag, and pitching-
moment coefficients for the sharp-nose cone.

Figure 11.- Variation with angle of attack of lift, drag, and pitching-
moment coefficients for the blunt-nose cone.
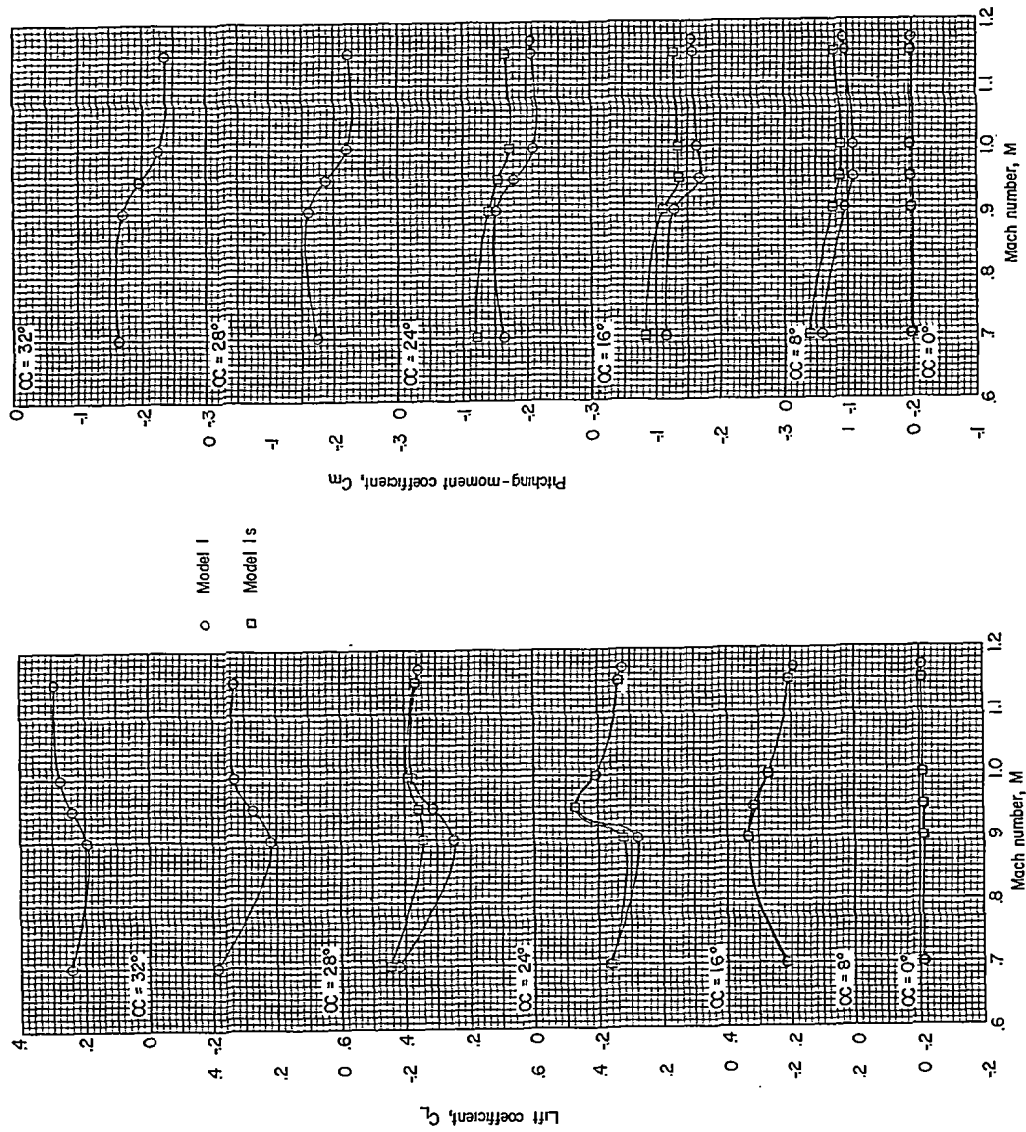
Figure 12.- Variation of lift and pitching-moment coefficients with Mach number in the transonic range for models 1 and 1s at selected angles of attack.
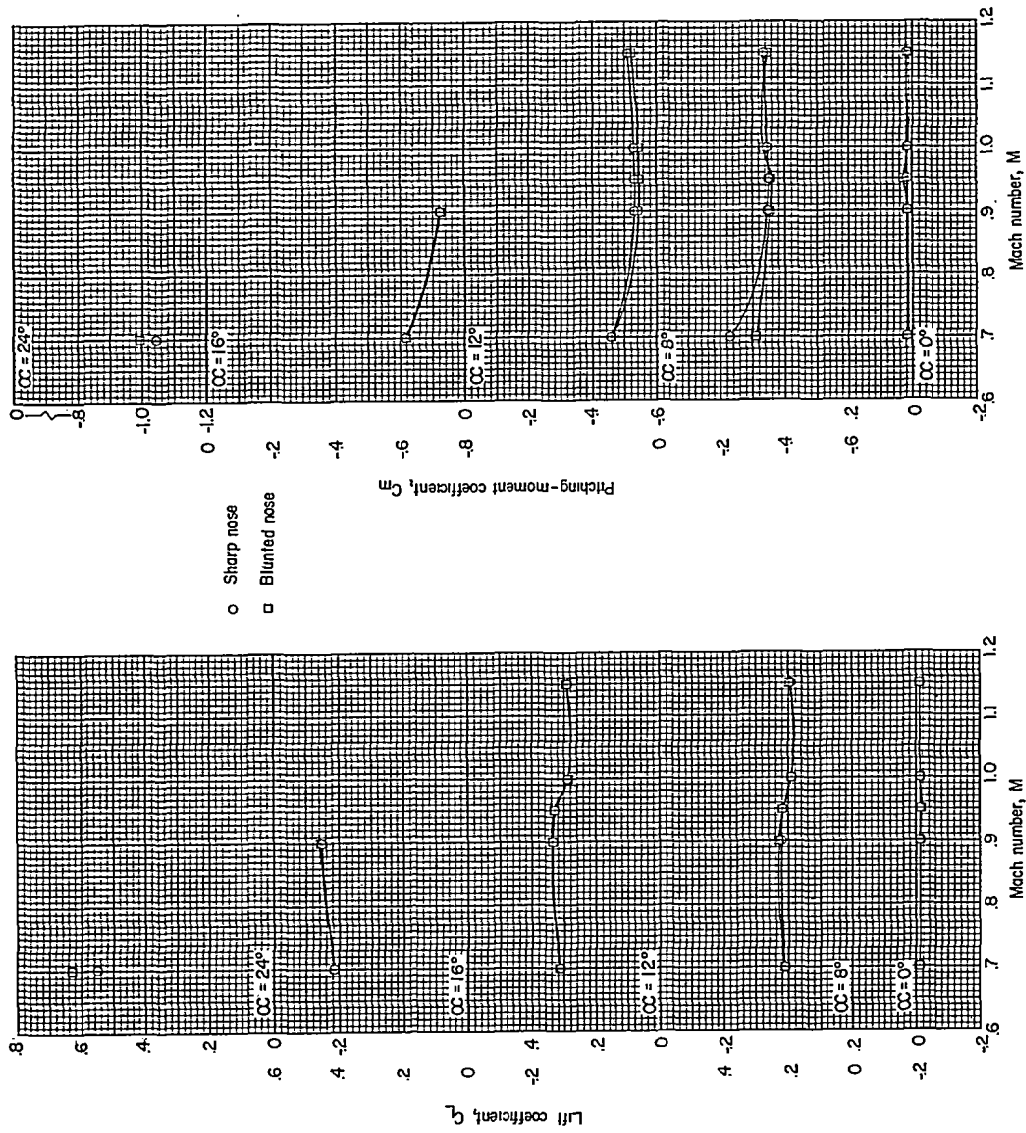
L-180

Model
3
3a
3b

Pitching-moment coefficient, C_m

Mach number, M

Lift coefficient, C_L
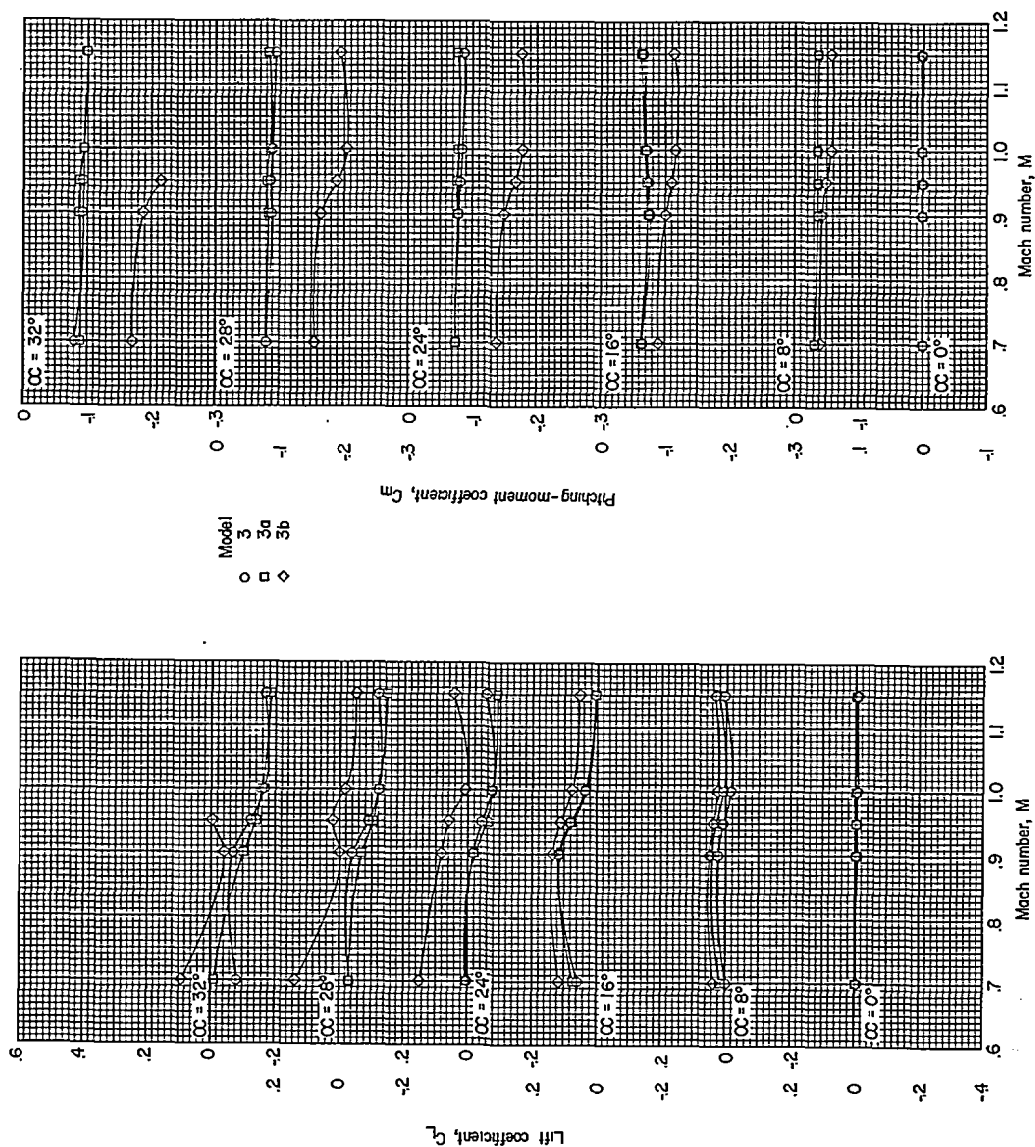
Mach number, M

Figure 13.- Variation of lift and pitching-moment coefficients with Mach number in the transonic range for models 3, 3a, and 3b at selected angles of attack.

Figure 14.- Variation of lift and pitching-moment coefficients with Mach number in the transonic range for the sharp- and blunted-nose cone models at selected angles of attack.
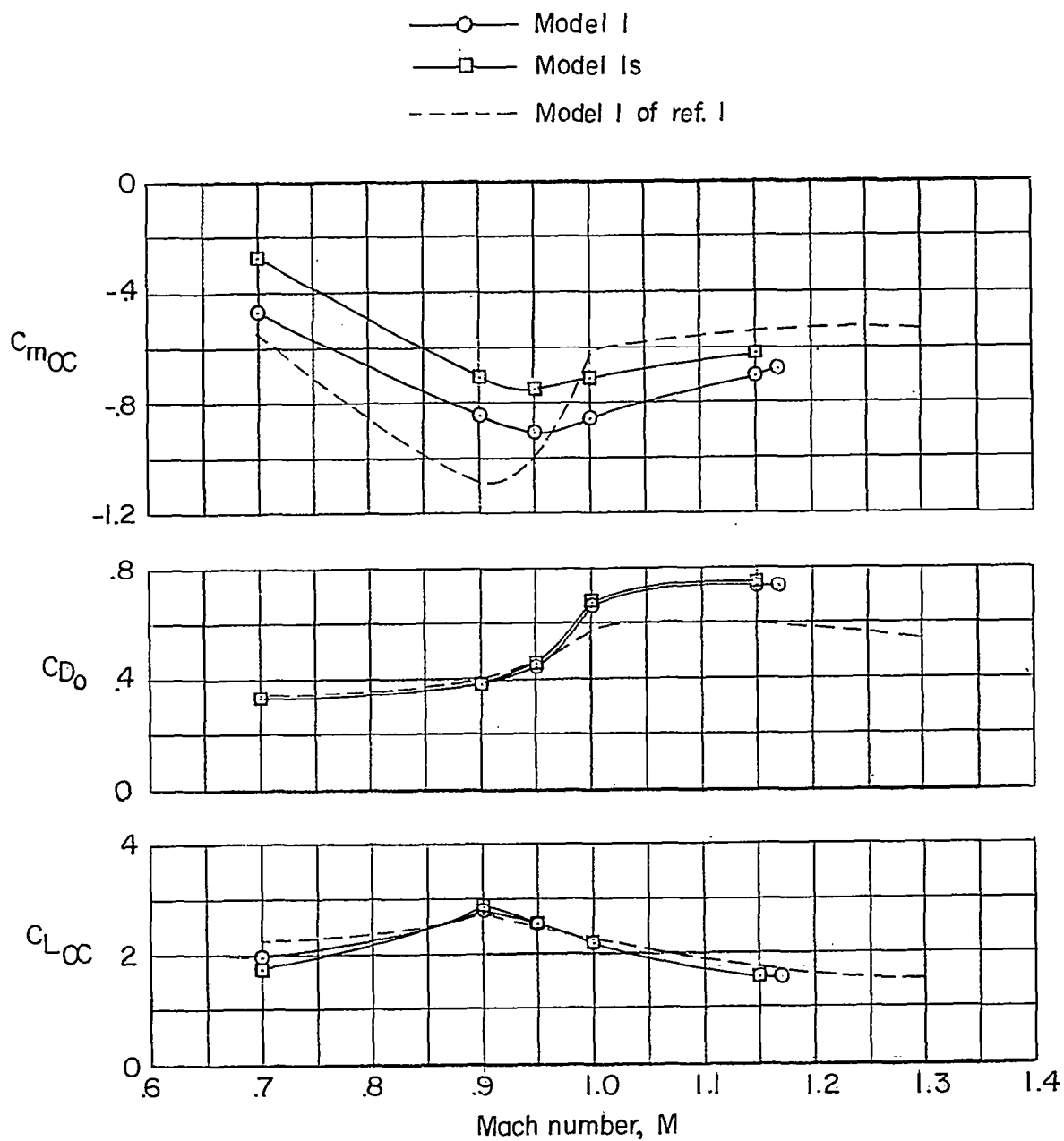
Figure 15.- Effect of Mach number on the aerodynamic derivatives for a full-skirted model.

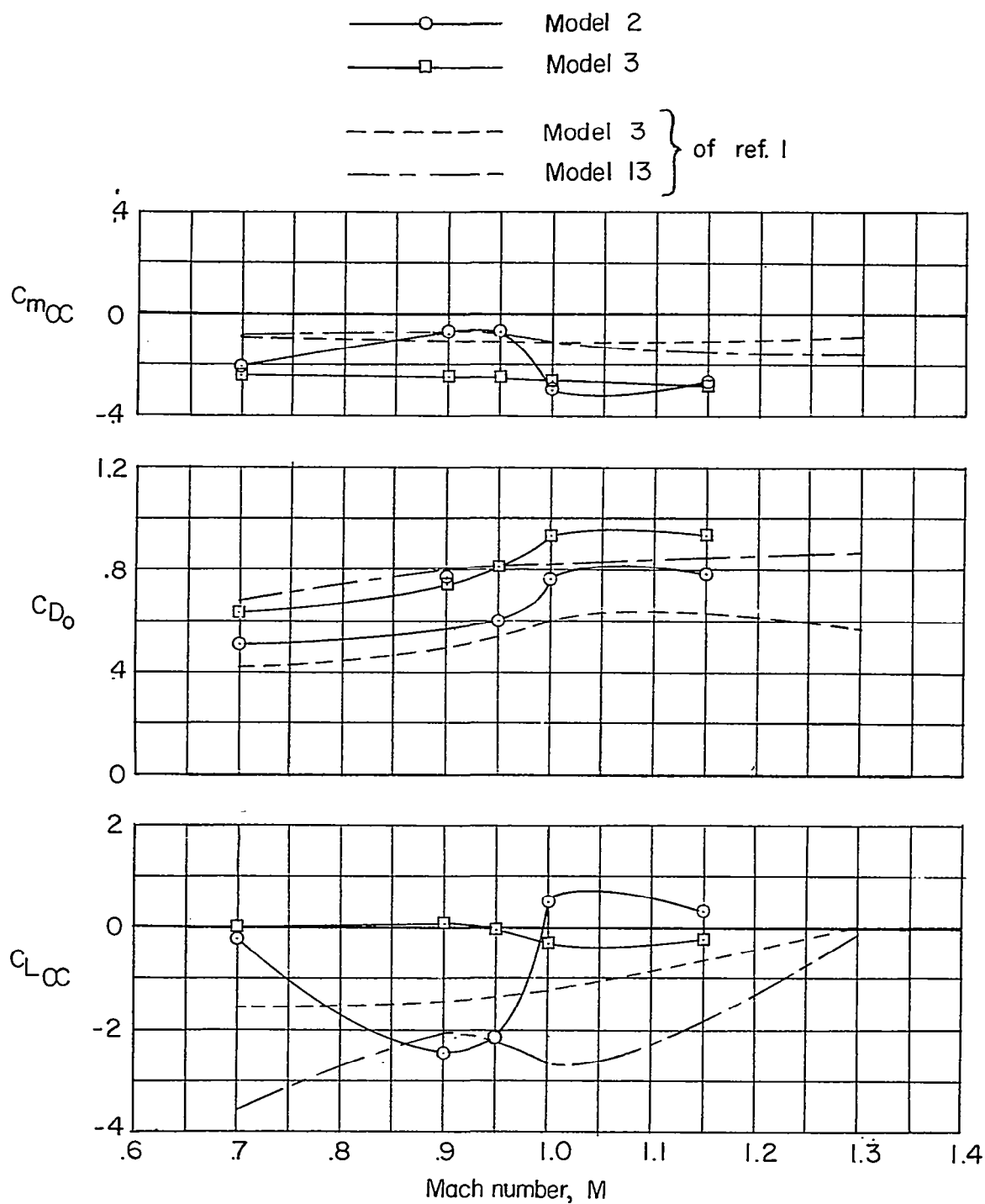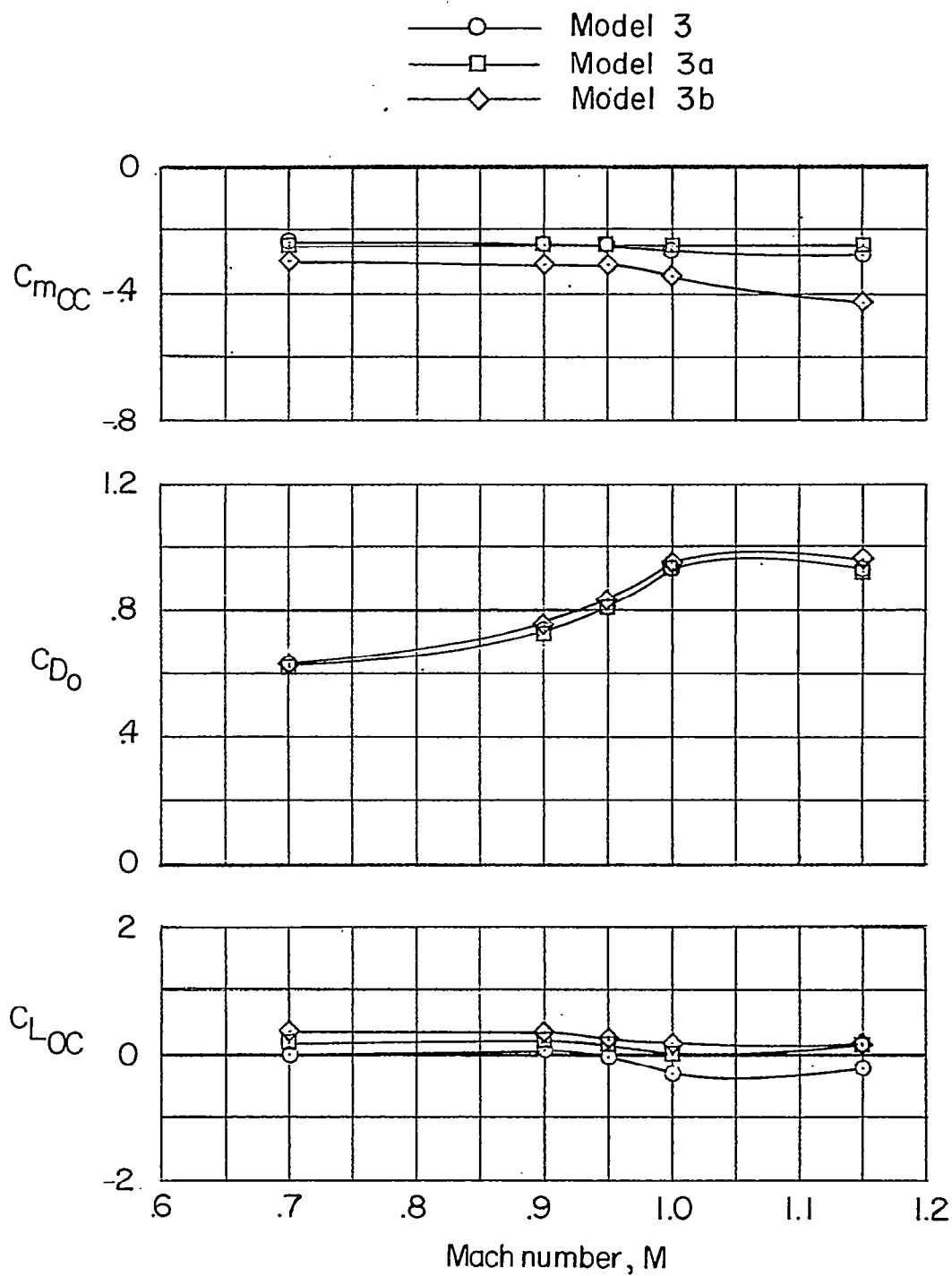Figure 16.- Effect of Mach number on the aerodynamic derivatives for short-skirted models.

L-180

Figure 17.- Effect of Mach number on the aerodynamic derivatives for a model with extendible afterbody flaps.

—o— Sharp cone
—□— Blunt cone
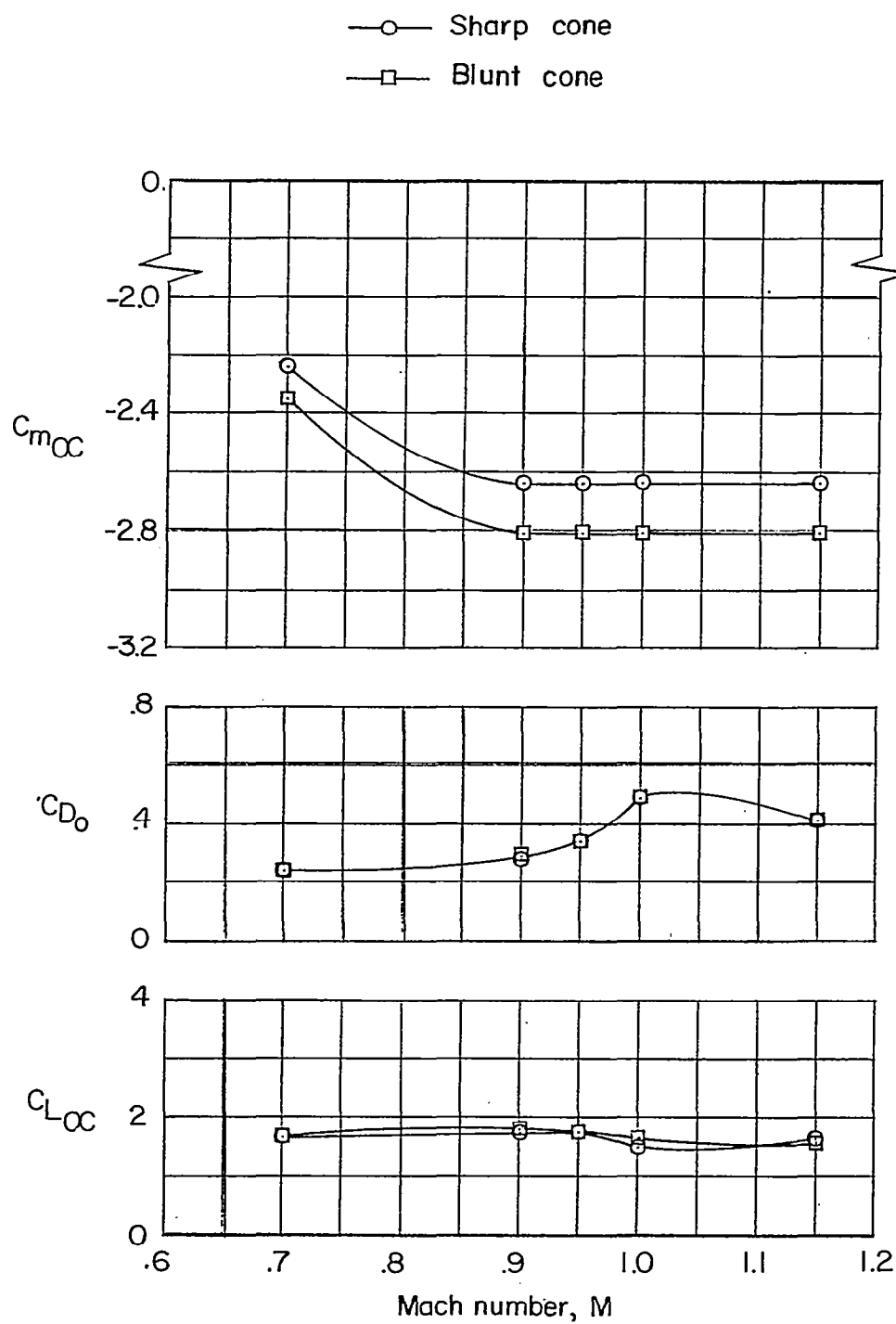

Figure 18.- Effect of Mach number on the aerodynamic derivatives for a
15° cone.